

Quantum Dots: Theory, Application, Synthesis

Pranjal Vachaspati*

Massachusetts Institute of Technology

(Dated: May 7, 2013)

Semiconductor crystals smaller than about 10 nm, known as quantum dots, have properties that differ from large samples, including a bandgap that becomes larger for smaller particles. These properties create several applications for quantum dots, including efficient solar cells and qubits for quantum computing. Various synthesis procedures have been proposed and implemented, including chemical synthesis and lithographic synthesis similar to that used in the semiconductor industry.

I. INTRODUCTION

Quantum dots were first characterized in 1983 by Brus[1] as small semiconductor spheres in a colloidal suspension. When the radius of a semiconductor sphere becomes small, on the order of a few nanometers, the Bohr radii of the charge carriers become larger than the sphere, and their confinement to the sphere causes their energy to increase.

This effect can be modeled in a number of ways. A straightforward method which we present here treats the quantum dot as a finite spherical potential well and incorporates both confinement effects and Coulomb attraction between charge carriers.

The easily tunable bandgap of quantum dots makes them especially suited for optical applications, including LEDs and photovoltaic cells. Additionally, their easily described behavior makes them useful as qubits, since excited electron spins in individual quantum dots can be precisely controlled electronically.

II. THEORY

A. Bulk Semiconductor Mechanics

The energy structure for a solid can be derived from a periodic-potential model. As seen in Figure 1, an insulator has a ground state that is totally filled, so applying an electric field does not cause a momentum change. In contrast, a conductor has a partially filled ground state, so adding an external electric field causes the electrons to shift into states with an overall non-zero momentum.

A semiconductor has a ground state (called the valence band) like that of an insulator, but the first excited state is very close to the ground state. Small excitations can lift electrons into the first excited state, known as the conduction band. This allows the excited electrons to move in the mostly empty conduction band, and the unexcited electrons to move in the now slightly empty valence band. The motion of the unexcited electrons can also be treated as the movement of a positively charged hole, which significantly simplifies calculations.

Electronic structure of
insulators, conductors, and semiconductors
No electric field Electric field

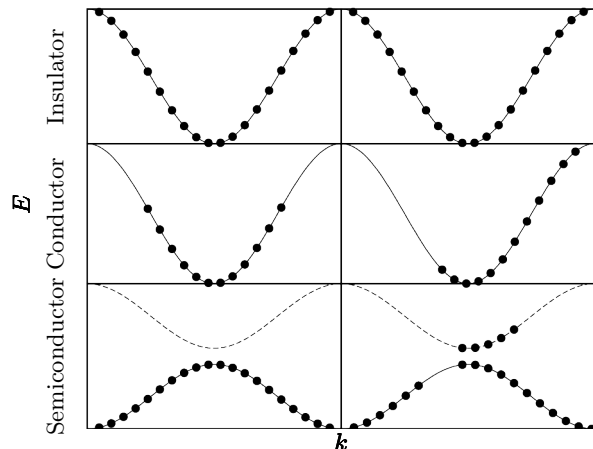


FIG. 1. When a solid is placed in an electric field, states with momentum in the direction of the field become more favorable. In an insulator, the valence band is totally filled, so the average momentum does not change. In a conductor, the valence band is only partially filled, so electrons can occupy more energetically favorable states with a net momentum. In a semiconductor, the valence band is full, but a band with only a slight energy gap is accessible, so particles can jump into this band and conduct.

Calculating the precise conduction band shape of a semiconductor is difficult, and using it can be unwieldy. However, for small momenta, the conduction band can be approximated by a parabola. This produces the “effective mass approximation” :

$$E = \frac{\hbar^2 k^2}{2m^*} \quad (1)$$

where m^* is called the effective mass of the carrier and depends on the curvature of the band. The effective mass of an electron is typically between $0.1m_e$ and m_e .

At some finite temperature T , the carrier wave vectors, k , are on average described by

$$\frac{3k_B T}{2} = \frac{\hbar^2 k^2}{2m^*} \quad (2)$$

For a semiconductor with $m^* = m_e$, the characteristic length scale is $1/k$, and is on the order of 10 nm. We

* pranjal@mit.edu

therefore investigate the behavior of semiconductor crystals below this size.

In general, the Hamiltonian of an electron-hole pair in a large semiconductor is given as

$$H = -\frac{\hbar^2}{2m_h}\nabla_h^2 - \frac{\hbar^2}{2m_e}\nabla_e^2 - \frac{e^2}{\epsilon|r_e - r_h|} \quad (3)$$

where ϵ is the dielectric constant. The first two terms represent the kinetic energies of the hole and the electron respectively, and the third term represents the Coulomb attraction between them.

B. Small Semiconductor Crystals

We next consider a small spherical semiconductor crystal with radius R . In a large semiconductor, the excitons may be treated as free-particles and the boundary conditions may be ignored, but for sufficiently small crystals, the Hamiltonian in Eq. 3 must be modified to take into account the fact that the semiconductor acts as a potential well. The modified Hamiltonian is

$$H = -\frac{\hbar^2}{2m_h}\nabla_h^2 - \frac{\hbar^2}{2m_e}\nabla_e^2 - \frac{e^2}{4\pi\epsilon|\vec{r}_e - \vec{r}_h|} + V_e + V_h \quad (4)$$

where V_e and V_h are zero inside the sphere and some positive constant V_0 , that depends on the medium the crystal is in, outside the sphere. The dielectric constant for the crystal is given by ϵ . For an infinite well, the confinement energy disregarding the Coulomb term is given by $\frac{\hbar^2\pi^2n^2}{2mR^2}$ as in a square well, and the electrostatic energy disregarding the confinement term is of order $\frac{e^2}{\epsilon R}$. As will be shown, the infinite square well approximation significantly overestimates the band gap for small quantum dots, so we must consider a finite spherical square well instead.

The inverse quadratic dependence on R in the confinement energy compared to the inverse linear dependence in the electrostatic energy means that in the small R limit, the confinement term dominates. Therefore, we first calculate the confinement energies and wavefunctions for a finite well, and treat the Coulomb energy as a perturbation on top of that.

We are calculating the properties of the first excited state, which is spherically symmetric and has no angular momentum. Thus, the wavefunction has no dependence on the spherical angles. The unperturbed confinement Hamiltonian for an electron or hole is given by

$$H = -\frac{\hbar^2}{2m}\nabla^2 + V(r) \quad (5)$$

Schrödinger's equation gives

$$-\frac{\hbar^2}{2m}\frac{1}{r^2}\frac{\partial}{\partial r}\left(r^2\frac{\partial\psi(r)}{\partial r}\right) + V(r)\psi(r) = E\psi(r) \quad (6)$$

Allowed values of k_{in}

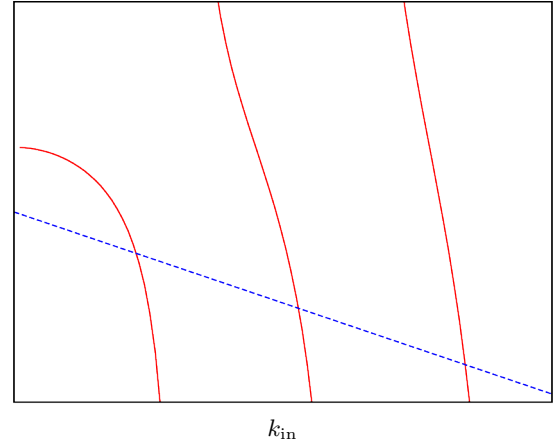


FIG. 2. Equation 14 is solved graphically to find valid electron momenta in the finite spherical well potential.

which simplifies to

$$\frac{2}{r}\frac{\partial\psi}{\partial r} + \frac{\partial^2\psi}{\partial r^2} = -\frac{2m(E - V(r))}{\hbar^2}\psi(r) \quad (7)$$

For clarity, we write

$$k_{out} = \sqrt{\frac{2m_0(E - V_0)}{\hbar^2}}; \quad k_{in} = \sqrt{\frac{2m^*E}{\hbar^2}} \quad (8)$$

The solutions to Equation 7 are Bessel functions. Inside the sphere, the wavefunction must be finite at the origin and therefore has the form

$$\psi(r) = A\frac{\sin k_{in}r}{k_{in}r}, \quad r < R \quad (9)$$

Outside, the wavefunction must converge to zero at large r , so the state has the form

$$\psi(r) = -B\frac{e^{-k_{out}r}}{k_{out}r}, \quad r > R \quad (10)$$

The probability current is preserved by [2]:

$$\frac{1}{m^*\psi_{in}(R)}\frac{d\psi_{in}(R)}{dr} = \frac{1}{m_0\psi_{out}(R)}\frac{d\psi_{out}(R)}{dr} \quad (11)$$

Substituting Equations 9 and 10 for ψ_{in} and ψ_{out} gives

$$\frac{1}{m^*}\left(-\frac{1}{R} + k_{in}\cot(k_{in}R)\right) = -\frac{1}{m_0}\frac{1 + k_{out}R}{R} \quad (12)$$

Following Equation 8, k_{out} is written in terms of k_{in} :

$$k_{out} = \frac{m_0}{m^*}\sqrt{k_{in}^2 - \frac{V_0}{\hbar^2 m^*}} \quad (13)$$

Equation 13 is then substituted into Equation 12:

$$k_{\text{in}}R \cot(k_{\text{in}}R) = 1 - \frac{m^*}{m_0} - \sqrt{\frac{m^*}{m_0} \left(R^2 k_{\text{in}}^2 + \frac{V_0 R^2 m^*}{\hbar^2} \right)} \quad (14)$$

Equation 14 can be solved numerically (Figure 2) to find valid values of k_{in} and therefore the wavefunctions and energy spectrum of the confined electron and hole.

We can account for the effect of electron-hole interactions by applying perturbation theory. The perturbation to the Hamiltonian is given by

$$\delta H = \frac{e^2}{4\pi\epsilon|r_e - r_h|} \quad (15)$$

so the first-order perturbation to the energy is given by

$$\delta E = \langle \psi_{e0}, \psi_{e1} | \frac{e^2}{4\pi\epsilon|\vec{r}_e - \vec{r}_h|} | \psi_{e0}, \psi_{e1} \rangle \quad (16)$$

$$\delta E = \frac{e^2}{4\pi\epsilon} \int \frac{\psi_h(\vec{r}_h)^2 \psi_e(\vec{r}_e)^2}{\sqrt{r_e^2 + r_h^2 - 2\vec{r}_e \cdot \vec{r}_h}} \sin\theta_h \sin\theta_e r_e^2 r_h^2 dr_e d\theta_e d\phi_e \quad (17)$$

This integral does not have a simple analytic solution, and must be evaluated numerically. In the large V_0 limit,

$$\delta E \approx \frac{1.8e^2}{4\pi\epsilon R}. \quad (18)$$

This perturbation becomes less significant as the dots become larger and the confinement potential V_0 becomes weaker.

C. Comparison of Experimental and Theoretical Results

To validate this theory, we compare successive levels of approximation to experimental results. For cadmium sulfide dots in an oleic acid solution, the confinement potential V_0 is 5 eV, the effective electron mass is $0.18m_e$, and the effective hole mass is $0.54m_e$. The infinite square well approximation (Figure 3) closely follows the finite square well approximation and experimental results for dots larger than about 2 nm, but diverges sharply for larger dots, overestimating the bandgap change for 0.5 nm dots by a factor of five.

The unperturbed finite well approximation (Figure 4) works well for all CdS dot sizes for which experimental data was available. The electron-hole interaction term improves the result slightly for small dots, and contributes around ten percent to the total energy. For more strongly confined dots, like indium phosphide, which has $V_0 = 1.83\text{eV}$, the Coulomb interaction can contribute as much as thirty percent.

Finally, this model is found to break down for narrow-bandgap semiconductors, including indium arsenide,

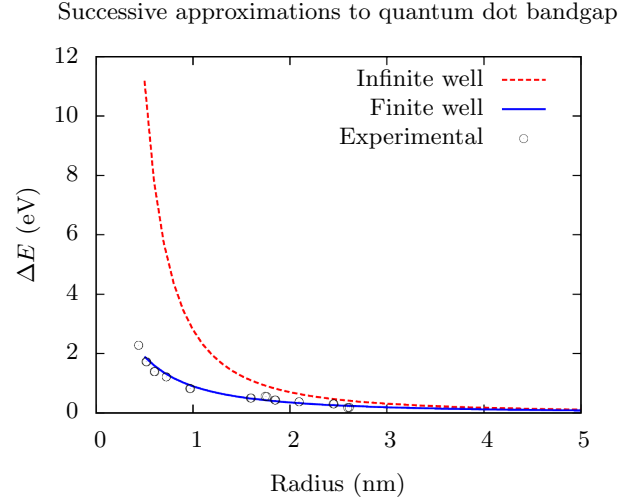


FIG. 3. The infinite square well approximation diverges significantly from the finite square well approximation and experimentally observed energies for small quantum dots. Experimental data from [3].

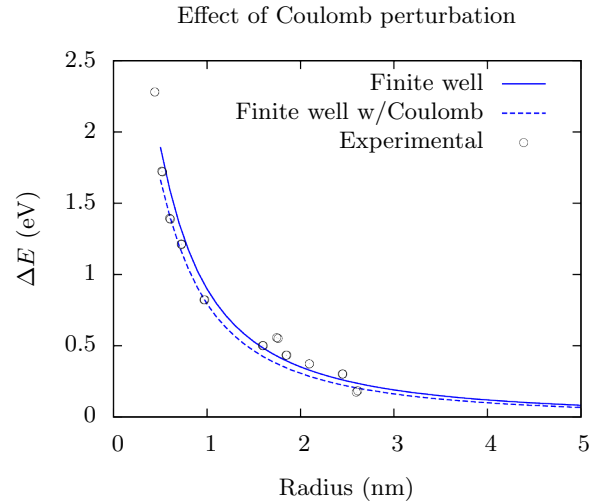


FIG. 4. The Coulomb perturbation is small for CdS, since the confinement potential ($V_0 = 1.25\text{eV}$) is relatively small. It is roughly ten percent the size of the confinement energy. Experimental data from [3].

which has a bandgap of 0.354 eV. In such semiconductors, the conduction band is highly non-parabolic, so the effective mass approximation breaks down. These semiconductors also have very large Bohr radii, so the confinement effect is very strong, and the large momentum pushes the excitons away from the parabolic edges of the bands [3].

III. APPLICATIONS

A. Solar Cells

A traditional solar cell consists of a large silicon p-n junction. When a photon with energy greater than the bandgap of silicon hits the solar cell, it excites a single electron with energy exactly equal to the silicon bandgap. Photons with energy less than the bandgap are transmitted by the silicon and do not contribute to the power output. This results in a bandgap-dependent voltage-current tradeoff. If the bandgap is lower, more incoming photons can excite electrons (higher current), but the electrons have lower energy (lower voltage). If the bandgap is higher, fewer incoming photons can excite electrons, but the electrons have higher energy.

The sun can be modeled as a black body with a temperature of 6000 K. The peak solar cell efficiency is a function of bandgap, and has a theoretical maximum of 33.7% [4]. In practice, silicon solar cells have reached this efficiency in research settings.

However, this limit applies only to single-junction, single-bandgap solar cells. To get around this, quantum dots of varying size can form layers on top of each other [5], with the largest bandgaps on top. Incoming photons will be transmitted by quantum dots with too-large bandgaps until they reach a layer with a bandgap smaller than their energy. Given enough layers, each photon will excite an electron with an energy very close to its own energy, and very little energy is wasted. In fact, in the infinite-layer limit, the efficiency approaches the thermodynamic limit of 86% [6].

B. Quantum Computing

Two nearby quantum dots, each with a single excited electron, have been used as a two-qubit system for quantum computation [7]. The system is placed in a uniform magnetic field, creating a splitting between the $|\downarrow\rangle$ and $|\uparrow\rangle$ electron states. The system can be initialized in the $|\uparrow\downarrow\rangle$ state by putting both electrons in a single well, which has a singlet state as the ground state. As the potential of the second well is lowered adiabatically, one of the electrons will move into that well, depending on the polarity of the magnetic field. Allowing a coupling between the two electrons then allows a \sqrt{SWAP} gate to be applied, which exchanges the $|\uparrow\downarrow\rangle$ and $|\downarrow\uparrow\rangle$ states when applied twice. This gate, when paired with single qubit operations, is known to be universal [8] – that is, it can be used to create any quantum circuit.

IV. SYNTHESIS

Because of the great utility of quantum dots as described in III, many methods of synthesis have been pro-

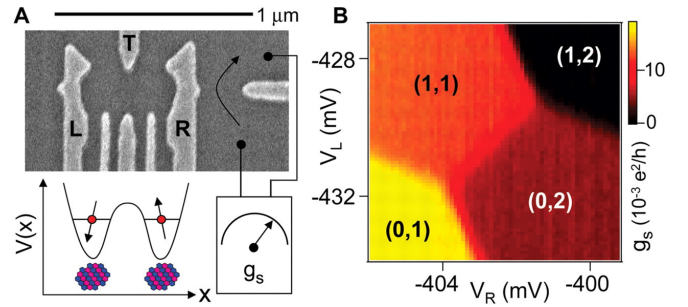


FIG. 5. Quantum dot qubits[7]: (A) shows the two adjacent quantum dots. Terminals L and R control the number of electrons in each of the dots. Terminal T controls the coupling between the electrons in the two dots. (B) shows the number of electrons in each dot as a function of the L and R terminal voltages.

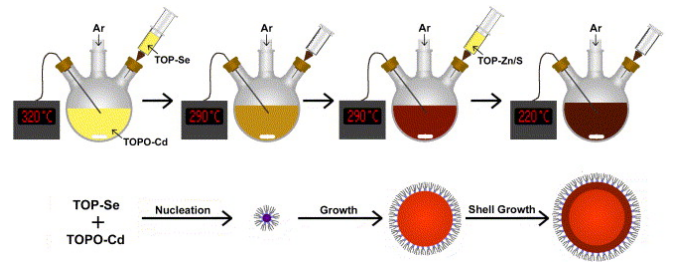


FIG. 6. Colloidal synthesis of CdSe[9]: A cadmium compound is heated to 320° C and dissolves in an organic solvent. A room temperature selenium compound dissolved in a different organic solvent is injected into the reaction vessel, causing supersaturation of the resultant CdSe solution. As the temperature drops to around 290° C, nucleation of new crystals stops and existing crystals grow. After a period of growth, the length of which determines the size of the quantum dots, the solution is cooled to 220° C, stopping growth. A small amount of zinc sulfide is injected into the reaction vessel to coat the quantum dots and prevent them from reacting with the environment.

posed and implemented. These vary greatly in terms of scalability, quality, and ease.

A. Chemical Assembly

1. Colloidal Synthesis

The most accessible technique for creating quantum dots is colloidal synthesis - that is, chemically producing quantum dots suspended in solution. One method for producing CdSe is shown in Figure 6, but a variety of chemical synthesis routes are possible for each semiconductor material. In general, a saturated solution of the semiconductor is produced in an organic solvent. Then the temperature or pH is changed to produce a supersaturated solution, which nucleates to produce small crystals.

The size of the resulting quantum dots can typically

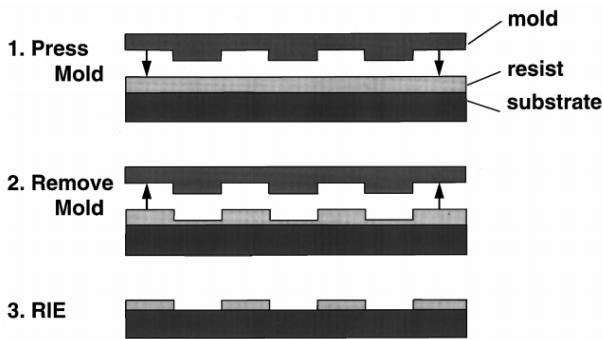


FIG. 7. Nanoimprint lithography [13]: A nanoscale mold is pressed into a semiconductor to create very small features.

be tuned by changing the temperature, pH, or length of the reactions. Most of these processes can be carried out in small quantities in the lab without requiring exotic reagents or equipment, although larger quantities can be difficult to produce as precise temperature control is required. Furthermore, the easiest semiconductors to make with this process (e.g. CdS, CdSe, CdTe) use cadmium, which is a heavy metal that is harmful to the environment and legally restricted in the European Union.

Colloidal synthesis also has a number of technical disadvantages. First of all, a separate reaction must be developed for each semiconductor material. Many of these reactions [10] require high temperatures or other inconvenient operations. The response of the particle size to reaction parameters like temperature and pH must be characterized. Colloidal synthesis also tends to produce a relatively wide size distribution of dots. The reactions typically produce size distributions of 10-15% of the desired size, but filtration and selection techniques can reduce that to 5% [11]. Colloidal synthesis is ill-suited for applications that require careful placement or manipulation of quantum dots, like quantum computing, but well-suited for applications that require large quantities of quantum dots, like solar cells.

B. Lithographic Assembly

Semiconductor lithography is typically used for the construction of integrated circuits. A semiconductor wafer is coated with a photosensitive “resist” material,

which is then covered with a stencil and exposed to ultraviolet light, which causes the parts exposed to light to harden. A development chemical, similar to those used for photography, then washes away the part of the resist that was not exposed to light. The wafer is then etched with a chemical such as hydrofluoric acid that attacks the semiconductor where it is not covered by resist. Photolithographic techniques are sometimes used for producing quantum dots [12], but the small size (~ 10 nm) desired in quantum dots can be hard to achieve with even high-frequency ultraviolet light.

Instead, a non-conventional form of lithography called imprint lithography is best suited for producing quantum dots [13]. Instead of etching a semiconductor wafer with light, a negative image is formed on a hard SiO_2 wafer using electron-beam lithography, a process similar to photolithography. This mold is used as a stamp and is physically pressed onto a silicon layer to form the quantum dots. This technique allows for precise positioning and size control of the quantum dots, and is being investigated for use in classical and quantum computing applications.

V. CONCLUSION

A simple finite well model has been shown to describe the size-dependent bandgap of quantum dots well for many materials. This model predicts a bandgap that increases significantly as dot size decreases. Applications of this effect to photovoltaic cells are very promising in increasing efficiency, provided that scalable manufacturing techniques can be developed. Finally, the utility of quantum dots as qubits in quantum computing has been investigated. The precise electronic control afforded over electron spins is promising for developing scalable quantum computing.

ACKNOWLEDGMENTS & NOTES

The author is grateful to Sabrina Pasterski and Daniel Kolodrubetz for comments in the course of writing this paper.

Mathematica code for approximating the bandgap of quantum dots will be made available at the author’s website (<http://pranj.al/quantumdots>).

[1] L. Brus, *The Journal of chemical physics* **79**, 5566 (1983).
 [2] S. Horiguchi, *Physica B: Condensed Matter* **227**, 336 (1996).
 [3] G. Pellegrini, G. Mattei, and P. Mazzoldi, *Journal of applied physics* **97**, 073706 (2005).
 [4] W. Shockley and H. J. Queisser, *Journal of Applied Physics* **32**, 510 (1961).

[5] K. W. Barnham and G. Duggan, *Journal of Applied Physics* **67**, 3490 (1990).
 [6] A. De Vos, *Journal of Physics D: Applied Physics* **13**, 839 (1980).
 [7] J. Petta, A. Johnson, J. Taylor, E. Laird, A. Yacoby, M. Lukin, C. Marcus, M. Hanson, and A. Gossard, *Science* **309**, 2180 (2005).

- [8] Y. Zhou, G.-F. Zhang, F.-H. Yang, and S.-L. Feng, arXiv preprint arXiv:0808.2549 (2008).
- [9] R. E. Bailey, A. M. Smith, and S. Nie, *Physica E: Low-dimensional Systems and Nanostructures* **25**, 1 (2004).
- [10] A. Guzelian, U. Banin, A. Kadavanich, X. Peng, and A. Alivisatos, *Applied physics letters* **69**, 1432 (1996).
- [11] C. B. Murray, S. Sun, W. Gaschler, H. Doyle, T. A. Betley, and C. R. Kagan, *IBM Journal of Research and Development* **45**, 47 (2001).
- [12] L. Zhuang, L. Guo, and S. Y. Chou, *Applied Physics Letters* **72**, 1205 (1998).
- [13] S. Y. Chou, P. R. Krauss, W. Zhang, L. Guo, and L. Zhuang, *Journal of Vacuum Science & Technology B: Microelectronics and Nanometer Structures* **15**, 2897 (1997).
- [14] D. Loss and D. P. DiVincenzo, *Physical Review A* **57**, 120 (1998).
- [15] L. E. Brus, *The Journal of chemical physics* **80**, 4403 (1984).
- [16] S. Y. Chou, P. R. Krauss, and P. J. Renstrom, *Journal of Vacuum Science & Technology B: Microelectronics and Nanometer Structures* **14**, 4129 (1996).
- [17] T. Rajh, O. I. Micic, and A. J. Nozik, *The Journal of Physical Chemistry* **97**, 11999 (1993).
- [18] J. Y. Marzin, J. M. Gérard, A. Izraël, D. Barrier, and G. Bastard, *Phys. Rev. Lett.* **73**, 716 (1994).
- [19] K. K. Nanda, F. E. Kruis, and H. Fissan, *Nano Letters* **1**, 605 (2001).
- [20] M. V. Rama Krishna and R. A. Friesner, *Phys. Rev. Lett.* **67**, 629 (1991).
- [21] J. Ferreyra and C. Proetto, *Physical Review B* **60**, 10672 (1999).